Journal of Materials Chemistry A

RSC Publishing

PAPER

Graphene-oxide-coated $LiNi_{0.5}Mn_{1.5}O_4$ as high voltage cathode for lithium ion batteries with high energy density and long cycle life†

Cite this: *J. Mater. Chem. A*, 2013, **1**, 4083

Xin Fang,[a] Mingyuan Ge,[a] Jiepeng Rong[a] and Chongwu Zhou*[b]

Lithium ion batteries are receiving enormous attention as power sources and energy storage devices in the renewable energy field. With the ever increasing demand for higher energy and power density, high voltage cathodes have emerged as an important option for new generation batteries. Here, we report graphene-oxide-coated $LiNi_{0.5}Mn_{1.5}O_4$ as a high voltage cathode and demonstrate that the batteries showed superior cycling performance for up to 1000 cycles. Mildly oxidized graphene oxide coating was found to improve the battery performance by enhancing the conductivity and protecting the cathode surface from undesired reactions with the electrolyte. As a result, the graphene-oxide-coated high voltage cathode $LiNi_{0.5}Mn_{1.5}O_4$ showed 61% capacity retention after 1000 cycles in the cycling test, which converts to only 0.039% capacity decay per cycle. At large current rates of 5 C, 7 C and 10 C, the batteries were able to deliver 77%, 66% and 56% of the 1 C capacity, respectively (1 C = 140 mA g^{-1}). In contrast, the $LiNi_{0.5}Mn_{1.5}O_4$ cathode without graphene oxide coating showed 88.7% capacity retention after only 100 cycles. The promising results demonstrated the potential of developing high energy density batteries with the high voltage cathode $LiNi_{0.5}Mn_{1.5}O_4$ and improving the battery performance by surface modification with mildly oxidized graphene oxide.

Received 17th December 2012
Accepted 24th January 2013

DOI: 10.1039/c3ta01534c

www.rsc.org/MaterialsA

Introduction

Since Sony first commercialized lithium ion batteries in the early 1990s, the market for lithium ion batteries has been rapidly growing with the increasing demand for energy storage systems. In spite of the great success of lithium ion battery technology developed for portable electronic devices, higher requirements are raised by electric vehicles (EVs), hybrid electric vehicles (HEVs), and plug-in hybrid electric vehicles (PHEVs) in aspects of higher energy/power density, better rate capability, longer cycle life, and lower cost.[1–4] As the specific energy density is calculated by $\int_0^Q V(q)\mathrm{d}q/wt$,[5] increasing the working voltage of lithium ion batteries has become one of the most important strategies to enhance the energy density.

As the voltage of a lithium ion battery is mainly determined by the cathode material, the research of cathode materials for new lithium ion batteries has become extremely crucial and has gained enormous attention. $LiNi_{0.5}Mn_{1.5}O_4$ was studied when people were developing the method of partially substituting Mn with other metal ions (Co^{3+}, Ge^{4+}, Zn^{2+}, Ni^{2+}, Mg^{2+}, Cr^{3+} and Cu^{2+}) to suppress the Jahn–Teller distortion in spinel $LiMn_2O_4$ in the early 1990s.[6–9] $LiNi_{0.5}Mn_{1.5}O_4$ was first reported as a 3 V cathode material by Amine *et al.* in 1996,[10] and the 4.7 V voltage plateau was discovered by Dahn *et al.* in 1997.[11] With a theoretical capacity of 146.7 mA h g^{-1} and a high working voltage of 4.7 V, $LiNi_{0.5}Mn_{1.5}O_4$ has 20% and 30% higher energy density than $LiCoO_2$ and $LiFePO_4$, respectively, thus becoming a potential candidate to be used in EVs in the future.[12–17]

However, the conductivity of $LiNi_{0.5}Mn_{1.5}O_4$ is relatively low.[18] In addition, it is difficult to maintain the electrochemical stability of the carbonate-based liquid electrolyte at such a high working voltage, and the interfacial side reaction between the high-voltage charged $LiNi_{0.5}Mn_{1.5}O_4$ and the liquid electrolyte causes serious capacity fading during cycling.[19,20] There is usually a small amount of Mn^{3+} ions existing in the crystal, and the Mn^{3+} ions are inclined to decompose into Mn^{2+} and Mn^{4+}. The Mn^{2+} ions are reported to have a tendency to dissolve into the electrolyte and further deposit on the surface of the anode, and the deposition subsequently increases the impedance of the battery and causes capacity fading.[21] A potential approach to overcome this problem is to modify the surface of $LiNi_{0.5}Mn_{1.5}O_4$ with a thin layer of coating material, which is a strategy that has been successfully used on a number of cathode and anode materials.[22–25] Previously, the effect of some coating materials, such as Au,[26] Ag,[27] Bi_2O_3,[28] BiOF,[20] ZnO,[19,29] ZrO_2,[30] ZrP_2O_7,[30] AlF_3,[31] conductive carbon,[18] and polyimide,[32] has been

[a]*Mork Family Department of Chemical Engineering and Materials Science, University of Southern California, Los Angeles, California 90089, USA*

[b]*Ming Hsieh Department of Electrical Engineering, University of Southern California, Los Angeles, California 90089, USA. E-mail: chongwuz@usc.edu; Fax: +1 213 821 5696; Tel: +1 213 740 4708*

† Electronic supplementary information (ESI) available: Cyclic voltammetry test of the electrolyte system of $LiPF_6$@EC + DMC. See DOI: 10.1039/c3ta01534c

studied and showed improvement in the performance of $LiNi_{0.5}Mn_{1.5}O_4$ to a certain degree. However, no long cycling result was reported, which makes it difficult to judge the effect of coating in the long run. Among the coating materials mentioned above, most of the metal oxide and metal fluoride coatings only worked as a protection shell, but could not enhance the electron conductivity of $LiNi_{0.5}Mn_{1.5}O_4$. It was found that Bi_2O_3 was converted to Bi metal during cycling, which can help with fast electron transfer, but the cycling stability was not sufficiently good due to the microstructural changes of Bi_2O_3 during the charge–discharge process.[28] Other groups reported the direct coating of metals, such as Au and Ag; however, the improvement of Ag coating was limited,[27] and Au even made the battery performance worse than before.[26] Conductive carbon coating can be a good choice, since it can work as a protection layer and also enhance the electron conductivity of $LiNi_{0.5}Mn_{1.5}O_4$. Although this strategy is effective on many other materials, it is difficult for $LiNi_{0.5}Mn_{1.5}O_4$ since a reduction atmosphere is needed for a carbon source to carbonize at high temperature, while $LiNi_{0.5}Mn_{1.5}O_4$ needs an oxygen atmosphere to avoid too many oxygen vacancies in the crystal. In the report on conductive carbon coating of $LiNi_{0.5}Mn_{1.5}O_4$,[18] only a slow charge rate was shown and the coulomb efficiency was low. In this regard, it is important to find an alternative coating material that can act as a protection layer and at the same time enhance the conductivity.

Recently, graphene and graphene oxide have been reported to improve cycling stability and rate performance in lithium ion batteries and lithium sulfur batteries.[33–41] Graphene and graphene oxide were reported to be a stable wrapping layer during the charge–discharge process. The conductivity and interaction with the active materials can be tuned *via* controlling the degree of oxidation of graphene. However, to the best of our knowledge, the effect of graphene oxide on the performance of $LiNi_{0.5}Mn_{1.5}O_4$ has not been reported, in spite of the importance of $LiNi_{0.5}Mn_{1.5}O_4$ as a representative high voltage cathode material. In this paper, we explored the potential of using mildly oxidized graphene oxide as a coating layer for the $LiNi_{0.5}Mn_{1.5}O_4$ cathode and got very promising results. The batteries showed only 0.039% capacity decay per cycle for up to 1000 cycles. At high charge–discharge rates of 5 C, 7 C and 10 C (1 C = 140 mA g^{-1}), 77%, 66% and 56% of the 1 C capacity can be retained, respectively. The results indicate that graphene-oxide-coated $LiNi_{0.5}Mn_{1.5}O_4$ showed excellent cycling stability and rate capability as a high voltage cathode material and thus has great potential for high energy density and long life lithium ion batteries.

Experimental

Materials synthesis

To produce $LiNi_{0.5}Mn_{1.5}O_4$, nickel acetate ($Ni(Ac)_2 \cdot 4H_2O$) and manganese acetate ($Mn(Ac)_2 \cdot 4H_2O$) were mixed at a molar ratio of Ni : Mn = 1 : 3 and milled in a mortar. The mixture was then heated to 500 °C at a heating rate of 3 °C min^{-1} and calcined at 500 °C for 5 hours. After cooling down naturally, lithium acetate ($LiAc \cdot 2H_2O$) was added to the mixture at a molar ratio of Li : Ni : Mn = 2.1 : 1 : 3 (5% excess Li source was added in order to make up for the volatilization of Li during calcination), and the mixture was heated to 500 °C for 5 hours once more. Then the mixture was milled and sintered at 900 °C for 10 hours followed by annealing at 700 °C for 10 hours.

Graphene oxide was prepared using the modified Hummers method[42] and the details can be found in the literature.[43] The solid content in the graphene oxide solution was 1 mg ml^{-1}. Then, the as-synthesized $LiNi_{0.5}Mn_{1.5}O_4$ powder was mixed with graphene oxide/ethanol solution at room temperature with moderate stirring. The weight ratio of graphene oxide and the as-synthesized $LiNi_{0.5}Mn_{1.5}O_4$ was 1 : 20. The mixture was subsequently annealed at 90 °C overnight to get rid of the residual solvent that may exist between the surface of $LiNi_{0.5}Mn_{1.5}O_4$ and the graphene oxide wrapping layer to enhance the surface interaction.

Electrochemical measurements

CR2032 coin cells were assembled with Li metal as counter electrodes. The weight ratio in the cathode is active material : poly(vinylidene fluoride) : carbon black = 8 : 1 : 1. The loading of the cathode active material was kept between 2 and 3 mg cm^{-2} for all batteries tested in this paper. A 1 M solution of $LiPF_6$ in ethylene carbonate (EC) and dimethyl carbonate (DMC) (1 : 1, w/w) was used as electrolyte. The batteries were cycled in the voltage range of 3.5–5 V. Cyclic voltammetry (CV) curves were tested at a scan rate of 0.05 mV s^{-1}. Electrochemical impedance spectra (EIS) were collected with an AC voltage of 5 mV amplitude in the frequency range of 100 kHz to 10 mHz.

Results and discussion

$LiNi_{0.5}Mn_{1.5}O_4$ can be prepared *via* a variety of methods, including solid state reaction,[38,44] co-precipitation,[45] molten salt method,[46] radiated polymer gel method,[47] thermal polymerization,[48] sol–gel method,[49] and spray pyrolysis.[50] Among these methods, solid state reaction and co-precipitation are most compatible with large scale synthesis which is essential for industrial applications. Compared to co-precipitation, solid state reaction does not involve waste water, so it is more environmentally friendly. In this work, we used a modified solid state reaction method[38] to synthesize $LiNi_{0.5}Mn_{1.5}O_4$ with potential to be adopted by industry. Fig. 1 shows the X-ray diffraction (XRD) pattern of the as-synthesized $LiNi_{0.5}Mn_{1.5}O_4$. The pattern corresponds to the cubic structure of spinel $LiNi_{0.5}Mn_{1.5}O_4$, which is in agreement with the literature.[51] According to a previous study,[52] $LiNi_{0.5}Mn_{1.5}O_4$ has two space groups: $Fd\bar{3}m$ and $P4_332$. In the $Fd\bar{3}m$ space group, Mn^{3+} exists due to O vacancies in the crystal, while in the $P4_332$ space group, all Mn ions are Mn^{4+}. Even though $LiNi_{0.5}Mn_{1.5}O_4$ was commonly used in the literature[16] and also in this paper, the actual formula of $LiNi_{0.5}Mn_{1.5}O_4$ with the $Fd\bar{3}m$ space group should be $LiNi_{0.5}Mn_{1.5}O_{4-\delta}$. In our study, the product obtained was $Fd\bar{3}m$ spinel, which can be seen from the charge–discharge curves with the presence of a small Mn^{3+} plateau. Although the disordered $Fd\bar{3}m$ spinel was reported to give better

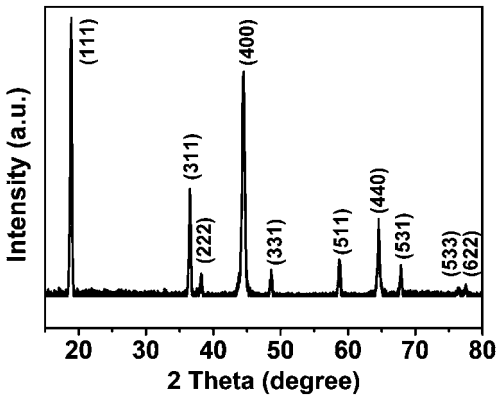

Fig. 1 X-ray diffraction pattern of as-synthesized $LiNi_{0.5}Mn_{1.5}O_4$.

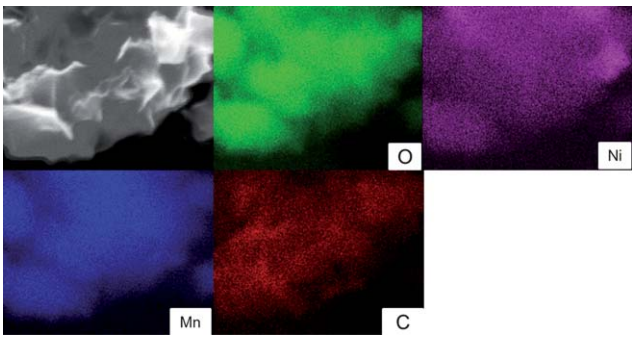

Fig. 3 EDX elemental mapping of graphene-oxide-coated $LiNi_{0.5}Mn_{1.5}O_4$. The upper left image shows the mapping area under SEM.

performance,[13,52] it encounters the problem of Mn^{3+} ion distortion and dissolution, which may get reduced and deposit on the surface of the anode. This will subsequently lead to increased impedance and capacity fading.

To modify the surface of $LiNi_{0.5}Mn_{1.5}O_4$ and protect it from undesired reactions, we coated the as-prepared $LiNi_{0.5}Mn_{1.5}O_4$ with mildly oxidized graphene oxide. Fig. 2 shows the scanning electron microscopy (SEM) and transmission electron microscopy (TEM) images of the as-synthesized $LiNi_{0.5}Mn_{1.5}O_4$ (Fig. 2a, c and e) and graphene-oxide-coated $LiNi_{0.5}Mn_{1.5}O_4$ (Fig. 2b, d and f). Fig. 2a and b correspond to the pristine and graphene-oxide-coated $LiNi_{0.5}Mn_{1.5}O_4$, respectively. The size of the $LiNi_{0.5}Mn_{1.5}O_4$ particles is mostly around 500 nm. While the TEM image of pristine $LiNi_{0.5}Mn_{1.5}O_4$ (Fig. 2c) shows a very clean surface, in comparison, it is evident in Fig. 2d that graphene oxide has been coated onto the outer surface of $LiNi_{0.5}Mn_{1.5}O_4$, with a thickness of about 5 nm. High resolution TEM (HRTEM) images (Fig. 2e and f) show the fine structure of $LiNi_{0.5}Mn_{1.5}O_4$ and the graphene oxide layer. In Fig. 2f, the layered stacking of graphene oxide can be clearly seen together with the $LiNi_{0.5}Mn_{1.5}O_4$ lattice, and there is no gap between graphene oxide and the $LiNi_{0.5}Mn_{1.5}O_4$ particle, indicating tight adhesion between graphene oxide and the $LiNi_{0.5}Mn_{1.5}O_4$ surface. Fig. 3 shows the energy dispersive X-ray spectroscopy (EDX) mapping of graphene-oxide-coated $LiNi_{0.5}Mn_{1.5}O_4$ under SEM (the SEM image on the top left side shows the mapping area). It is obvious that the mapping of element C, which is from graphene oxide, has the same distribution as elements Ni, Mn and O. This indicates that our graphene oxide is uniformly coated onto $LiNi_{0.5}Mn_{1.5}O_4$ particles.

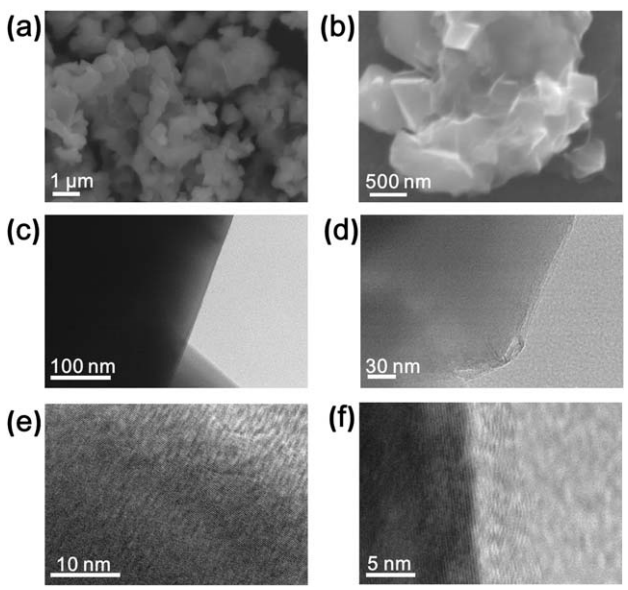

Fig. 2 (a) SEM image of as-synthesized $LiNi_{0.5}Mn_{1.5}O_4$. (b) SEM image of graphene-oxide-coated $LiNi_{0.5}Mn_{1.5}O_4$. (c) TEM image showing the surface of as-synthesized $LiNi_{0.5}Mn_{1.5}O_4$. (d) TEM image of graphene-oxide-coated $LiNi_{0.5}Mn_{1.5}O_4$. (e) HRTEM image of as-synthesized $LiNi_{0.5}Mn_{1.5}O_4$ showing the fine lattice. (f) HRTEM image of graphene-oxide-coated $LiNi_{0.5}Mn_{1.5}O_4$ showing the $LiNi_{0.5}Mn_{1.5}O_4$ lattice together with the layered stacking of graphene oxide on the surface.

To evaluate the electrochemical performance of graphene-oxide-coated $LiNi_{0.5}Mn_{1.5}O_4$, CR2032 coin cells were assembled with Li metal as counter electrodes. As a comparison, pristine $LiNi_{0.5}Mn_{1.5}O_4$ was also tested in the same condition. The results are shown in Fig. 4. The charge–discharge curves in Fig. 4a show the high working voltage feature of $LiNi_{0.5}Mn_{1.5}O_4$. Compared to other traditional cathode materials, such as $LiCoO_2$ (3.9 V), $LiMn_2O_4$ (4.1 V), and $LiFePO_4$ (3.5 V), a high working voltage of 4.7 V means that higher energy density can be achieved when $LiNi_{0.5}Mn_{1.5}O_4$ is used as a cathode for lithium ion batteries. By comparing the charge–discharge curves of pristine and graphene-oxide-coated $LiNi_{0.5}Mn_{1.5}O_4$, it is obvious that after graphene oxide coating, the voltage difference between charge and discharge plateaus gets smaller. This indicates that graphene oxide coating can help to reduce the polarization and inner resistance of the batteries. There is a small voltage plateau around 4.1 V, which can be attributed to the redox couple of Mn^{3+}/Mn^{4+}. The small plateau here confirms our analysis that the Ni and Mn ions should be disorderly distributed in the crystal structure, and the $LiNi_{0.5}Mn_{1.5}O_4$ particles we produced should possess the $Fd\bar{3}m$ space group.

Cyclic voltammetry (CV) curves of graphene-oxide-coated $LiNi_{0.5}Mn_{1.5}O_4$ shown in Fig. 4b are in good agreement with our charge–discharge curves. The main peaks are in the high voltage range, while the small peaks at 4–4.1 V correspond to the existence of Mn^{3+}. The integrated area of the 4 V peaks is much

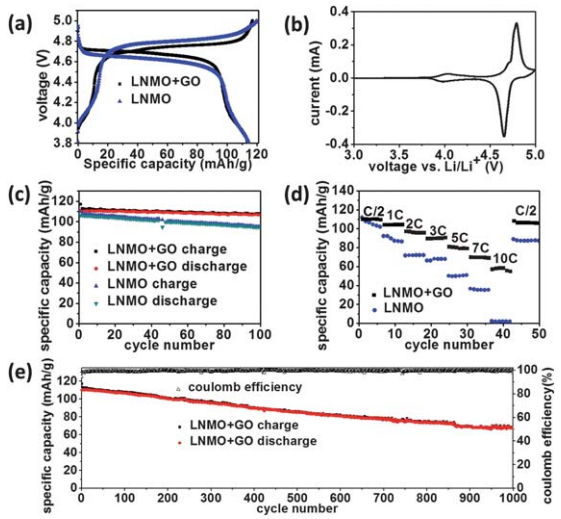

Fig. 4 (a) Charge–discharge curves of pristine $LiNi_{0.5}Mn_{1.5}O_4$ (denoted by LNMO) and graphene-oxide-coated $LiNi_{0.5}Mn_{1.5}O_4$ (denoted by LNMO + GO) at a current of C/5. (b) CV curves of graphene-oxide-coated $LiNi_{0.5}Mn_{1.5}O_4$ at a scan rate of 0.05 mV s^{-1}. (c) Comparison of cyclability of pristine $LiNi_{0.5}Mn_{1.5}O_4$ and graphene-oxide-coated $LiNi_{0.5}Mn_{1.5}O_4$ at C/2. (d) Discharge capacity of graphene-oxide-coated $LiNi_{0.5}Mn_{1.5}O_4$ and pristine $LiNi_{0.5}Mn_{1.5}O_4$ at different current rates; the charge current was kept at C/2. (e) The long cycling result of graphene-oxide-coated $LiNi_{0.5}Mn_{1.5}O_4$ at C/2.

smaller than that of the 4.7 V peaks, meaning that the main contribution of the total capacity and the total energy is from the Ni^{2+}/Ni^{4+} redox couple. There is no other peak in Fig. 4b, indicating that graphene oxide does not lead to extra redox reactions in the testing voltage range, and thus should remain stable and does not contribute to the capacity.

Fig. 4c shows the cycling performance of the pristine $LiNi_{0.5}Mn_{1.5}O_4$ (denoted by LNMO) and graphene-oxide-coated $LiNi_{0.5}Mn_{1.5}O_4$ (denoted by LNMO + GO) in comparison (the specific capacity of graphene-oxide-coated $LiNi_{0.5}Mn_{1.5}O_4$ was calculated using the total weight of graphene oxide and $LiNi_{0.5}Mn_{1.5}O_4$). It is observed that the coated $LiNi_{0.5}Mn_{1.5}O_4$ showed a more stable cycling performance than the uncoated $LiNi_{0.5}Mn_{1.5}O_4$ as a cathode in lithium ion batteries. The results from current rate capability tests are shown in Fig. 4d. When discharged at large current densities of 5 C, 7 C, and 10 C, the graphene-oxide-coated $LiNi_{0.5}Mn_{1.5}O_4$ can still deliver 77%, 66%, and 56% of the 1 C capacity, respectively. At each stage of the current rate test, the batteries showed excellent stability and no obvious degradation. When the current density went back to C/2, the capacity recovered to the original value, indicating that large current density and rapid lithiation/delithiation did not lead to any permanent damage to the crystal structure. In comparison, once the batteries were tested under large current densities, especially 10 C, it is evident that pristine $LiNi_{0.5}Mn_{1.5}O_4$ cannot get fully lithiated/delithiated due to large inner resistance, so the capacity decreased immediately. In addition, the capacity could not recover when the current density went back. This supports our analysis that graphene oxide can improve the conductivity and reduce the inner resistance of the cathode material. The long cycling result of graphene-oxide-coated $LiNi_{0.5}Mn_{1.5}O_4$ is shown in Fig. 4e. After cycling at C/2 (1 C = 140 mA g^{-1}) for 1000 cycles, the capacity retention of the graphene-oxide-coated $LiNi_{0.5}Mn_{1.5}O_4$ is 61%, meaning only 0.039% capacity decay per cycle. We attribute this improvement to the increased conductivity and the protection effect from mildly oxidized graphene oxide on the surface. The remarkable cycling and current rate performance from the graphene-oxide-coated $LiNi_{0.5}Mn_{1.5}O_4$ cathode indicates its potential for application in next-generation lithium ion batteries with high energy density, long cycle life, and good rate capability.

The performance of our graphene oxide coating compares favorably with other coatings reported in the literature. As mentioned before, metal oxide and metal fluoride coatings, such as Al_2O_3 and AlF_3, can only work as a protection layer, but cannot enhance the conductivity. On the other hand, Ag coating only led to limited improvement, while Au coating even made the battery performance worse than before. Although carbon coating showed the most promising result, only 92% capacity retention was achieved even with the best coating ratio. In contrast, we have achieved a long cycle life of 1000 cycles with our graphene-oxide-coated $LiNi_{0.5}Mn_{1.5}O_4$. In addition, the first 100 cycles showed over 96% capacity retention.

The promising performance caused by graphene oxide coating can be ascribed to three reasons. First of all, graphene oxide coating enhanced the conductivity of $LiNi_{0.5}Mn_{1.5}O_4$. With continuous graphene oxide coating, the $LiNi_{0.5}Mn_{1.5}O_4$ particles were interconnected with each other, and hence the conductivity was enhanced and the inner resistance was reduced. The modified Hummers method we used yielded mildly oxidized graphene oxide. It was reported to be low-defect graphene oxide,[43] which was important for conductivity. In addition, the existence of oxygenated groups rendered the mildly oxidized graphene oxide highly miscible with $LiNi_{0.5}Mn_{1.5}O_4$ particles when mixed in ethanol, and this way, the interaction of the graphene oxide and $LiNi_{0.5}Mn_{1.5}O_4$ particles was enhanced and the wrapping was more effective. Second, Mn^{3+} dissolution was suppressed due to graphene oxide coating. It was reported in the literature that Mn^{3+} ions had a tendency to undergo a disproportionation reaction and dissolve into the electrolyte.[53–56] This dissolution can cause destruction of the cathode crystal and thus affect the stability of the batteries. With the protection from graphene oxide coating, the dissolution of Mn^{3+} ions was suppressed and in this way the cycling stability was improved. Third, graphene oxide coating helped to reduce side reactions between Ni^{4+} ions and the electrolyte. Ni^{4+} ions, formed at the charged state of the cathode, were reported to be active towards the electrolyte and even raised safety concerns.[57] In addition, Ni ions were also found to dissolve into the electrolyte and further deposit onto the surface of the anode.[21,45] Since neither Mn nor Ni had good Li ion conductivity, the deposited layer increased the impedance of the batteries and caused capacity fading problem. It was also reported that the thickness of the products of undesired reactions, such as $Li_xPF_yO_z$ and $ROCO_2M$ (M = metal) species, increased with cycling and also caused capacity fading.[58] Hence, a protective surface layer like graphene oxide would be highly desired to improve the performance.

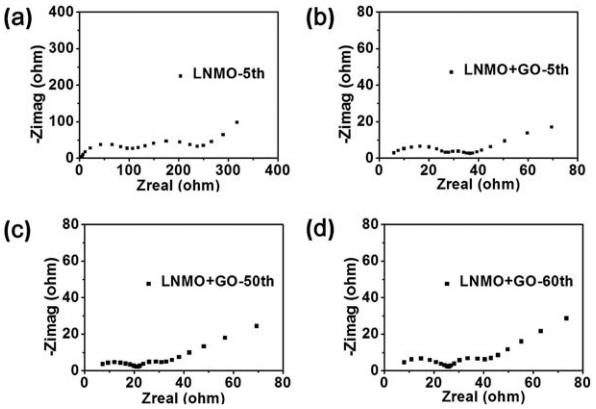

Fig. 5 AC impedance test results of (a) pristine $LiNi_{0.5}Mn_{1.5}O_4$ (denoted by LNMO) at the 5th cycle, (b) graphene-oxide-coated $LiNi_{0.5}Mn_{1.5}O_4$ (denoted by LNMO + GO) at the 5th cycle, (c) graphene-oxide-coated $LiNi_{0.5}Mn_{1.5}O_4$ at the 50th cycle and (d) graphene-oxide-coated $LiNi_{0.5}Mn_{1.5}O_4$ at the 60th cycle.

To confirm our analysis, electrochemical impedance spectra (EIS) were collected with an AC voltage of 5 mV amplitude in the frequency range of 100 kHz to 10 mHz. Fig. 5a and b show the AC impedance test results for pristine $LiNi_{0.5}Mn_{1.5}O_4$ and graphene-oxide-coated $LiNi_{0.5}Mn_{1.5}O_4$ at the 5th cycle, respectively. It can be clearly seen that the impedance of graphene-oxide-coated $LiNi_{0.5}Mn_{1.5}O_4$ is much smaller than that of the uncoated sample. This result supports our analysis that graphene oxide can help to reduce the impedance and thus improve the battery performance. We also further investigated the impedance of the graphene-oxide-coated $LiNi_{0.5}Mn_{1.5}O_4$ after the long cycling test and the results are shown in Fig. 5c and d. After 50 and 60 cycles, no obvious increase in battery impedance was observed. Even after long cycling, the impedance of graphene-oxide-coated $LiNi_{0.5}Mn_{1.5}O_4$ was still smaller than that of pristine $LiNi_{0.5}Mn_{1.5}O_4$, thus demonstrating the advantage of graphene oxide coating in improving the battery performance.

Conclusions

We successfully synthesized the high voltage cathode $LiNi_{0.5}Mn_{1.5}O_4$ *via* a highly scalable method of solid state reaction, and further modified the surface of $LiNi_{0.5}Mn_{1.5}O_4$ by graphene oxide coating. The high working voltage of 4.7 V gives the lithium ion batteries 20% and 30% higher energy density compared to batteries using traditional $LiCoO_2$ and $LiFePO_4$, respectively. The continuous graphene oxide coating provided better protection against interfacial side reactions between $LiNi_{0.5}Mn_{1.5}O_4$ surface and the electrolyte than previously reported discontinuous metal oxide coating. As a result, the graphene-oxide-coated $LiNi_{0.5}Mn_{1.5}O_4$ showed remarkable performance as a cathode for high energy and long life lithium ion batteries. For up to 1000 cycles, the batteries showed only 0.039% capacity decay per cycle. When discharged at large current rates of 5 C, 7 C, and 10 C, the batteries can still deliver 77%, 66%, and 56% of the 1 C capacity. The AC impedance test confirmed our analysis that graphene oxide coating helped to reduce the impedance of the battery and hence improved the battery performance. The graphene oxide coating reported in this work demonstrated a new method for enhancing the high voltage cathode performance and showed promising results for developing high energy density lithium ion batteries to be used for portable electronics, HEVs, PHEVs, and EVs in the future.

References

1 J. M. Tarascon and M. Armand, *Nature*, 2001, **414**, 359.
2 T. H. Kim, J. S. Park, S. K. Chang, S. Choi, J. H. Ryu and H. K. Song, *Adv. Energy Mater.*, 2012, **2**, 860.
3 M. Armand and J. M. Tarascon, *Nature*, 2008, **451**, 652.
4 L. W. Ji, Z. Lin, M. Alcoutlabi and X. W. Zhang, *Energy Environ. Sci.*, 2011, **4**, 2682.
5 J. B. Goodenough and Y. Kim, *J. Power Sources*, 2011, **196**, 6688.
6 J. M. Tarascon, E. Wang, F. K. Shokoohi, W. R. Mckinnon and S. Colson, *J. Electrochem. Soc.*, 1991, **138**, 2859.
7 R. Bittihn, R. Herr and D. Hoge, *J. Power Sources*, 1993, **43**, 223.
8 R. J. Gummow, A. Dekock and M. M. Thackeray, *Solid State Ionics*, 1994, **69**, 59.
9 T. Ohzuku, S. Takeda and M. Iwanaga, *J. Power Sources*, 1999, **81–82**, 90.
10 K. Amine, H. Tukamoto, H. Yasuda and Y. Fujita, *J. Electrochem. Soc.*, 1996, **143**, 1607.
11 Q. M. Zhong, A. Bonakdarpour, M. J. Zhang, Y. Gao and J. R. Dahn, *J. Electrochem. Soc.*, 1997, **144**, 205.
12 J. Hassoun, S. Panero, P. Reale and B. Scrosati, *Adv. Mater.*, 2009, **21**, 4807.
13 K. M. Shaju and P. G. Bruce, *Dalton Trans.*, 2008, 5471.
14 J. Hassoun, K. S. Lee, Y. K. Sun and B. Scrosati, *J. Am. Chem. Soc.*, 2011, **133**, 3139.
15 H. G. Jung, M. W. Jang, J. Hassoun, Y. K. Sun and B. Scrosati, *Nat. Commun.*, 2011, **2**, 516.
16 J. Xiao, X. L. Chen, P. V. Sushko, M. L. Sushko, L. Kovarik, J. J. Feng, Z. Q. Deng, J. M. Zheng, G. L. Graff, Z. M. Nie, D. W. Choi, J. Liu, J. G. Zhang and M. S. Whittingham, *Adv. Mater.*, 2012, **24**, 2109.
17 L. Zhou, D. Y. Zhao and X. W. Lou, *Angew. Chem., Int. Ed.*, 2012, **51**, 239.
18 T. Y. Yang, N. Q. Zhang, Y. Lang and K. N. Sun, *Electrochim. Acta*, 2011, **56**, 4058.
19 R. Alcantara, M. Jaraba, P. Lavela and J. L. Tirado, *J. Electroanal. Chem.*, 2004, **566**, 187.
20 H. B. Kang, S. T. Myung, K. Amine, S. M. Lee and Y. K. Sun, *J. Power Sources*, 2010, **195**, 2023.
21 Y. Talyosef, B. Markovsky, G. Salitra, D. Aurbach, H. J. Kim and S. Choi, *J. Power Sources*, 2005, **146**, 664.
22 S. T. Myung, K. Amine and Y. K. Sun, *J. Mater. Chem.*, 2010, **20**, 7074.
23 Y. Yao, N. Liu, M. T. McDowell, M. Pasta and Y. Cui, *Energy Environ. Sci.*, 2012, **5**, 7927.
24 Y. Yang, G. H. Yu, J. J. Cha, H. Wu, M. Vosgueritchian, Y. Yao, Z. A. Bao and Y. Cui, *ACS Nano*, 2011, **5**, 9187.
25 M. Y. Ge, J. P. Rong, X. Fang and C. W. Zhou, *Nano Lett.*, 2012, **12**, 2318.

26 J. Arrebola, A. Caballero, L. Hernan, J. Morales, E. R. Castellon and J. R. R. Barrado, *J. Electrochem. Soc.*, 2007, **154**, A178.
27 J. Arrebola, A. Caballero, L. Hernan, J. Morales and E. R. Castellon, *Electrochem. Solid-State Lett.*, 2005, **8**, A303.
28 J. Liu and A. Manthiram, *Chem. Mater.*, 2009, **21**, 1695.
29 Y. K. Sun, Y. S. Lee, M. Yoshio and K. Amine, *Electrochem. Solid-State Lett.*, 2002, **5**, A99.
30 H. M. Wu, I. Belharouak, A. Abouimrane, Y. K. Sun and K. Amine, *J. Power Sources*, 2010, **195**, 2909.
31 J. G. Li, Y. Y. Zhang, J. J. Li, L. Wang, X. M. He and J. Gao, *Ionics*, 2011, **17**, 671.
32 J. H. Cho, J. H. Park, M. H. Lee, H. K. Song and S. Y. Lee, *Energy Environ. Sci.*, 2012, **5**, 7124.
33 H. L. Wang, L. F. Cui, Y. A. Yang, H. S. Casalongue, J. T. Robinson, Y. Y. Liang, Y. Cui and H. J. Dai, *J. Am. Chem. Soc.*, 2010, **132**, 13978.
34 H. L. Wang, Y. Yang, Y. Y. Liang, L. F. Cui, H. S. Casalongue, Y. G. Li, G. S. Hong, Y. Cui and H. J. Dai, *Angew. Chem., Int. Ed.*, 2011, **50**, 7364.
35 X. F. Zhou, F. Wang, Y. M. Zhu and Z. P. Liu, *J. Mater. Chem.*, 2011, **21**, 3353.
36 H. L. Wang, Y. Yang, Y. Y. Liang, J. T. Robinson, Y. G. Li, A. Jackson, Y. Cui and H. J. Dai, *Nano Lett.*, 2011, **11**, 2644.
37 L. W. Ji, M. M. Rao, H. M. Zheng, L. Zhang, Y. C. Li, W. H. Duan, J. H. Guo, E. J. Cairns and Y. G. Zhang, *J. Am. Chem. Soc.*, 2011, **133**, 18522.
38 X. Y. Feng, C. Shen, X. Fang and C. H. Chen, *J. Alloys Compd.*, 2011, **509**, 3623.
39 J. S. Chen, Z. Y. Wang, X. C. Dong, P. Chen and X. W. Lou, *Nanoscale*, 2011, **3**, 2158.
40 J. X. Zhu, T. Zhu, X. Z. Zhou, Y. Y. Zhang, X. W. Lou, X. D. Chen, H. Zhang, H. H. Hng and Q. Y. Yan, *Nanoscale*, 2011, **3**, 1084.
41 M. Zhang, D. N. Lei, X. Z. Yu, L. B. Chen, Q. H. Li, Y. G. Wang, T. H. Wang and G. Z. Cao, *J. Mater. Chem.*, 2012, **22**, 23091.
42 W. S. Hummers and R. E. Offeman, *J. Am. Chem. Soc.*, 1958, **80**, 1339.
43 Y. X. Xu, K. X. Sheng, C. Li and G. Q. Shi, *J. Mater. Chem.*, 2011, **21**, 7376.
44 X. Fang, Y. Lu, N. Ding, X. Y. Feng, C. Liu and C. H. Chen, *Electrochim. Acta*, 2010, **55**, 832.
45 X. Fang, N. Ding, X. Y. Feng, Y. Lu and C. H. Chen, *Electrochim. Acta*, 2009, **54**, 7471.
46 J. H. Kim, S. T. Myung and Y. K. Sun, *Electrochim. Acta*, 2004, **49**, 219.
47 H. Y. Xu, S. Xie, N. Ding, B. L. Liu, Y. Shang and C. H. Chen, *Electrochim. Acta*, 2006, **51**, 4352.
48 G. B. Zhong, Y. Y. Wang, Z. C. Zhang and C. H. Chen, *Electrochim. Acta*, 2011, **56**, 6554.
49 H. Liu, Y. P. Wu, E. Rahm, R. Holze and H. Q. Wu, *J. Solid State Electrochem.*, 2004, **8**, 450.
50 S. H. Park and Y. K. Sun, *Electrochim. Acta*, 2004, **50**, 431.
51 P. Strobel, A. I. Palos, M. Anne and F. Le Cras, *J. Mater. Chem.*, 2000, **10**, 429.
52 J. H. Kim, S. T. Myung, C. S. Yoon, S. G. Kang and Y. K. Sun, *Chem. Mater.*, 2004, **16**, 906.
53 G. Amatucci and J. M. Tarascon, *J. Electrochem. Soc.*, 2002, **149**, K31.
54 D. Aurbach, M. D. Levi, K. Gamulski, B. Markovsky, G. Salitra, E. Levi, U. Heider, L. Heider and R. Oesten, *J. Power Sources*, 1999, **81–82**, 472.
55 Y. Y. Xia, Y. H. Zhou and M. Yoshio, *J. Electrochem. Soc.*, 1997, **144**, 2593.
56 M. M. Thackeray, *Prog. Solid State Chem.*, 1997, **25**, 1.
57 Y. K. Sun, S. T. Myung, B. C. Park, J. Prakash, I. Belharouak and K. Amine, *Nat. Mater.*, 2009, **8**, 320.
58 H. Duncan, Y. Abu-Lebdeh and I. J. Davidson, *J. Electrochem. Soc.*, 2010, **157**, A528.